Bachelor thesis

Excitonic energy transfer with long-range interactions

Can it be realized in ultracold Rydberg gases?

Sebastian Weber

September 16, 2013

5. Physikalisches Institut
Universität Stuttgart

Prof. Dr. Tilman Pfau
Dr. Sebastian Hofferberth
Dr. Robert Löw

Declaration

I hereby declare that I wrote this bachelor thesis on my own. To the best of my knowledge and belief, it contains no material previously published or written by another person, except where due acknowledgment has been made in the text.

Sebastian Weber

Stuttgart, September 16, 2013

Zusammenfassung

Der quantenmechanische Transport von Information beziehungsweise Energie durch Netzwerke ist das Thema vieler Veröffentlichungen. Aktuell wird zum Beispiel daran geforscht, wie Informationen mit Hilfe von Spin-Systemen effektiv transportiert werden können [1, 2]. Auch Photosynthese betreibende Organismen erfahren zur Zeit viel Aufmerksamkeit. Sie besitzen Lichtsammelkomplexe, die die Energie von absorbiertem Licht zu Reaktionszentren leiten. Neue Forschungen zeigen, dass dieser Energietransport sehr effektiv und kohärent erfolgt [3]. In dieser Bachelorarbeit geht es um den Transport von Anregungen. Alle diese Transportphänomene sind miteinander verwandt. Wenn man eines analysiert, lernt man in der Regel auch etwas über die anderen. In den meisten Fällen kann der Transport vereinfacht durch Modelle beschrieben werden, die dem Bose-Hubbard Modell [4] ähneln.

Dieser Ansatz wird auch in der vorliegenden Arbeit verfolgt. In dieser werden Netzwerke betrachtet, die aus mehreren bosonischen Zwei-Niveau-Systemen bestehen. Zunächst befindet sich ein einziges dieser Systeme in dem angeregten Zustand. Durch Wechselwirkung zwischen den Systemen breitet sich dann die Anregung quantenmechanisch im gesamten Netzwerk aus. Das im Verlauf dieser Bachelorarbeit entwickelte Simulationsprogramm ermöglicht zu analysieren, wie sich unterschiedliche Netzwerkgeometrien und Wechselwirkungspotenziale auf die Ausbreitung der Anregung auswirken.

Hierzu werden zunächst sehr einfache, kleine Netzwerke und dann Gitter untersucht. Es ergeben sich unter anderem die folgenden Ergebnisse: Je mehr Nachbarn ein angeregtes Teilchen hat, desto schneller wird es von einem Teil der Anregung verlassen. Andererseits steigt der zurückbleibende Anteil ebenfalls mit der Nachbarzahl. Auch die Positionierung der Nachbarn hat einen großen Einfluss. So führt zum Beispiel die Anisotropie von quadratischen Gittern mit Dipol-Dipol-Wechselwirkung zu einer Anregungsausbreitung über die Diagonalen. Es stellt sich heraus, dass schon kleinste Positionsänderungen der Gitterteilchen einen großen Einfluss auf die Ausbreitungen haben.

Um das Simulationsprogramm zu überprüfen, werden analytisch Dispersionsrelationen für unendlich lange, lineare Ketten hergeleitet. Diese stimmen gut mit den Dispersionsrelationen überein, die aus den Simulationsergebnissen berechnet werden. Dass hierbei nur endlich viele Teilchen verwendet worden sind, führt dazu, dass nur diskrete Wellenvektoren auftreten. Außerdem divergiert die Dispersionsrelation für mit $1/R$ abfallende Wechselwirkungen nicht. Dispersionsrelationen können auch zu einem besseren Verständnis der Anregungsausbreitung beitragen. Zum Beispiel zeigt sich, dass sie für kubische Gitter nur für kleine Wellenvektoren isotrop sind. Dies führt dazu, dass sich auf kubischen Gittern nur breit verteilte Anregungen isotrop ausbreiten.

Zum Schluss wird geprüft, ob es machbar ist, den Anregungstransport mit Superatomen zu untersuchen. Diese sind Cluster von Atomen, die sich eine Rydberg-Anregung teilen. Es zeigt sich, dass dies prinzipiell möglich ist. Jedoch muss man den Durchmesser der Superatome im Verhältnis zu ihrem Abstand klein halten, da es ansonsten zu einer schnellen Dephasierung kommt.

Abstract

This thesis deals with the simulation of networks of non-radiatively interacting bosons. The coupling between the bosons causes excitations to propagate.

Our numerical implementation allows us to analyze arbitrary two-dimensional patterns coupled by nearest neighbor interaction or $1/R^\alpha$-potentials. We study how crucially the propagation of excitations depends on network geometries and interaction potentials. To gain a better understanding of observed phenomena, several dispersion relations are extracted from simulation data. A comparison with analytically calculated dispersion relations reveals finite-size effects. The analytic results are also used to validate the simulation program.

As a specific implementation of such coupled networks, we investigate systems of Rydberg excitations. We analyze how promising the approach is, to experimentally study energy transfer with the help of so-called superatoms. It becomes apparent that their physical extension causes dephasing.

Contents

1 Introduction

Motivation

Quantum networks that transfer information respectively energy are subjects to active research.

- The transfer of quantum information through spin systems is a current topic. One goal is to improve the transport efficiency [1, 2].
- The study of quantum energy transport in biologic systems, such as photosynthetic bacteria (see figure 1), has received huge attention in the last few years, even though the basic principles were firstly discussed more than 80 years ago [5]. Not long ago evidence for wavelike energy transfer through quantum coherence was found [3].

All of these networks are related to each other. Hence, if we investigate one of them we will learn about the others. One common approach is to describe them with the help of models that are similar to the Bose-Hubbard model [4]. This model was originally designed for “hopping” bosons, but it also describes “hopping” information or energy. Another similarity between some of these processes is, that they can be seen as quantum walks. Quantum walks allow quantum algorithms which are much faster than their classical counterparts [6]. Quite recently it was shown, that multiparticle quantum walk is capable of universal quantum computation [7].

In this bachelor thesis we look at networks consisting of bosonic two level systems. We suppose that they interact non-radiatively in such a way that excitations are transfered. This process can be analyzed with the help of Rydberg gases. The long time goal of our research is to better understand the excitonic energy transfer observed in biologic systems. This thesis can be considered as a first step. As a side effect we also learn about the related networks mentioned above. At several passages of this thesis we are going to refer to them.

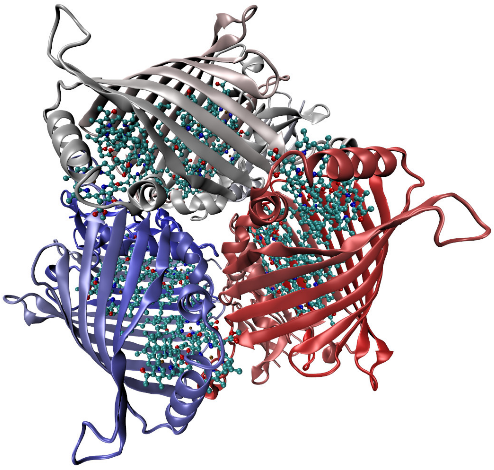

Fig. 1: Light harvesting protein of a green sulfur bacteria [8].

Outline of this thesis

First, we develop a general model of the propagation of excitations in chapter 2. During the course of the bachelor thesis we have programmed a software that efficiently calculates the time evolution. We make use of this software to analyze the propagation in various networks with various interaction potentials.

In chapter 3 we investigate three types of networks. We start with the type that is most simple to understand and end with the most complicated one.

- At first we analyze networks consisting of few particles which can be understood easily.
- Afterwards we look at regular lattices and study how anisotropy affects the propagation.
- Finally we take a short glance at irregular networks.

In chapter 4 we analytically calculate dispersion relations and compare them with simulation results to validate our simulation procedure. Hereby we learn about finite size effects on dispersion relations. Additionally, dispersion relations help us a to understand the spread of excitations.

In chapter 5 we study the feasibility of implementing such transfer networks in ultracold Rydberg gases with so-called superatoms.

2 The model

In this chapter, we develop a model for the propagation of excitations in networks.

A quantum system with a finite number of sites is considered. Each site is occupied by exactly one bosonic particle that can be in the quantum state $|0\rangle$ or $|1\rangle$. At the beginning of the simulation one or more particles are excited to $|1\rangle$ with a certain probability. The particles will interact if and only if they are in different states. The interaction will be non-radiative.

This general system is studied in the following. In chapter 5 we get more specific. There, we are going to use so called superatoms as particles to build up the system.

2.1 Schrödinger equation

Because we are only interested in coherent processes, the time evolution of the system can be obtained by solving the Schrödinger equation. To avoid numerical errors due to very huge or small numbers atomic units are used.

$$i\frac{\mathrm{d}}{\mathrm{d}t}|\Psi(t)\rangle = H\ |\Psi(t)\rangle \tag{1}$$

As we will see in the next section the Hamilton operator is time-independent, so that the solution can be easily determined.

$$|\Psi(t)\rangle = e^{-iHt}\ |\Psi(0)\rangle \tag{2}$$

To calculate the matrix exponential e^{-iHt} we diagonalize the Hamilton operator. Because it is Hermitian, it can be diagonalized by a unitary matrix. Let us assume the Hamilton operator has the eigenvalue and eigenvector pairs (λ_i, v_i). Then the solution of the Schrödinger equation can be written as follows.

$$|\Psi(t)\rangle = \begin{pmatrix} v_1 & \cdots \end{pmatrix} \begin{pmatrix} e^{-i\lambda_1 t} & \\ & \ddots \end{pmatrix} \begin{pmatrix} v_1 & \cdots \end{pmatrix}^* |\Psi(0)\rangle \tag{3}$$

Here, M^* is the conjugate transpose of the matrix M.

2.2 Hamilton operator

Without interaction, a system containing one excited particle is in a state that is an eigenvector of the Hamiltonian. With interaction, this is no longer the case and the state is not a stationary solution of the Schrödinger equation any more. Hence, the probability of finding a particle in an excited state will change over time. In the following we going to determine the Hamilton operator that describes the time evolution.

We will say that there is an excitation at site a, if the particle at this site is in the state $|1\rangle$. From this point of view, the interaction of particles causes hopping of excitations. This way of speaking allows us to perform calculations in the Fock space of the excitations, that is created by a very simple basis set.

- It owns the basis elements $|n_1, ...n_a, ..., n_N\rangle$.
- The occupancy number $n_a \in \{0, 1\}$ tells, whether there is an excitation at site a.

The idea of hopping excitations suggests that our system can be described by a Hamilton operator, that is similar to the Hamiltonian of the Bose-Hubbard model [4], like we said in chapter 1.

$$H_{\mathrm{BH}} = -t \sum_{\langle n,m\rangle} c_n^\dagger c_m + \frac{U}{2} \sum_n c_n^\dagger c_n (c_n^\dagger c_n - 1) \tag{4}$$

Here, $\langle n, m\rangle$ represents nearest neighbor interaction. We extend this to arbitrary interaction by replacing the simple hopping constant t with a function of n and m. Additionally the first sum has to include all combinations of sites.

Moreover we have to ensure that excitations can not be at the same site (hard-core bosons). In principle, this can be achieved by setting the on-site repulsion constant U to infinity. However, we do not need to do this, since our Fock space does not permit more than one excitation at the same site. Therefore we can neglect the addend containing U. By doing so we achieve the following interaction Hamilton operator.

$$H_i = \sum_{n\neq m} t(n, m)\; c_n^\dagger c_m \tag{5}$$

The creation $c_n^\dagger$ and annihilation operators c_n operate in the Fock space of the excitations. In the following $R_{nm} = |x_n - x_m|$ is the distance between the two sites n and m. We consider various explicit interaction types:

- $t(n, m) = t(\delta_{n-m-1} + \delta_{n-m+1})$: nearest neighbor interaction in 1D
- $t(n, m) = t/{R_{nm}}^6$: van der Waals interaction
- $t(n, m) = t/{R_{nm}}^3$: dipol-dipol interaction
- $t(n, m) = t/R_{nm}$: coulomb interaction

Our considerations have led to a very general interaction Hamilton operator 5 that fits many systems. In chapter 5 we are going to prove exemplarily, that we have chosen the correct Hamilton operator by canonical quantization of dipole-dipole interaction.

In general the interaction Hamilton operator 5 is not sufficient to describe systems. One has to add the Hamilton operator H_e containing the energies of the states on its diagonal. For systems containing one specific number of excitations all entries on the diagonal have the same value. Thus H_e is proportional to the identity matrix I, so that $H_e = k\ I$. Therefore it commutes with the interaction Hamilton operator H_i and the following calculation can be performed (matrices are printed in bold).

$$\begin{aligned} \left|\ |\Psi(t)\rangle\ \right|^2 &= \left|\ e^{-i(\boldsymbol{H_e}+\boldsymbol{H_i})t}\ |\Psi(0)\rangle\ \right|^2 = \left|\ e^{-i(k\boldsymbol{I}+\boldsymbol{H_i})t}\ |\Psi(0)\rangle\ \right|^2 \\ &= \left|\ e^{-ik\boldsymbol{I}t} e^{-i\boldsymbol{H_i}t}\ |\Psi(0)\rangle\ \right|^2 = \left|e^{-ikt} e^{-i\boldsymbol{H_i}t}\ |\Psi(0)\rangle\ \right|^2 \\ &= \left|e^{-i\boldsymbol{H_i}t}\ |\Psi(0)\rangle\ \right|^2 \end{aligned} \tag{6}$$

Hence, H_e can be neglected for these systems.

In the end we are interested in the probability of finding an excitation at a certain site. To calculate this quantity one has to use the single excitation basis. Let $|\Psi(t)_a\rangle$ be the wave function at the site a. Than the probability equals $\langle\Psi(t)_a|\Psi(t)_a\rangle$. Experimentally, a method distinguishing between the two states is required. In the case of Rydberg excitations, one can for example use state selective field ionization.

2.2.1 Example

As an example we are going to derive the Hamilton operator of a system that has the shape of an equilateral triangle, see figure 2. We suppose that each side has the length $a = 1$. Then all types of interactions lead to the same result because of the special geometry.

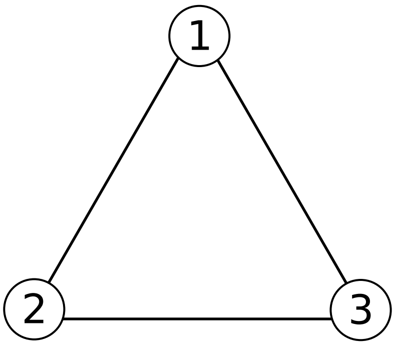

Fig. 2: An equilateral triangle with one particle at each corner is an example of a simple system. The lines show the coupling.

To express the Hamilton operator as a matrix, we need the basis elements of the Fock space. Restricting the available states of the system to one or two simultaneous excitations, the available Fock space can be constructed with the following basis elements.

$$\text{Basis} = \{|0,0,1\rangle, |0,1,0\rangle, |1,0,0\rangle, |0,1,1\rangle, |1,0,1\rangle, |1,1,0\rangle\} \tag{7}$$

The system has the following Hamilton operator where E is the energetic difference between the states $|0\rangle$ and $|1\rangle$.

$$H = t\begin{pmatrix} E & 1 & 1 & 0 & 0 & 0 \\ 1 & E & 1 & 0 & 0 & 0 \\ 1 & 1 & E & 0 & 0 & 0 \\ 0 & 0 & 0 & 2E & 1 & 1 \\ 0 & 0 & 0 & 1 & 2E & 1 \\ 0 & 0 & 0 & 1 & 1 & 2E \end{pmatrix} = t\begin{pmatrix} H_1 & \\ & H_2 \end{pmatrix} \tag{8}$$

As we can see, the Hamilton operator is sparse. It is composed of two blocks H_1 and H_2 on the diagonal. Thus the Schrödinger equation separates into two independent differential equations, which can be solved separately.

It is interesting, that instead of seeing interacting particles one can view figure 2 as the cycle graph C_3. The continuous-time quantum walk on this graph can be described by H_1 [9].

2.3 Simulation method

In the course of this thesis, the numerical solution of the model described above was implemented in `C++`. The resulting program enables the study of arbitrary two-dimensional patterns coupled by different $1/R^\alpha$-potentials. A graphical user interface is constructed with the `Qt` framework, see figure 3. For matrix and vector calculations the library `Eigen 3` is used. The patterns are drawn with the help of `OpenGL`.

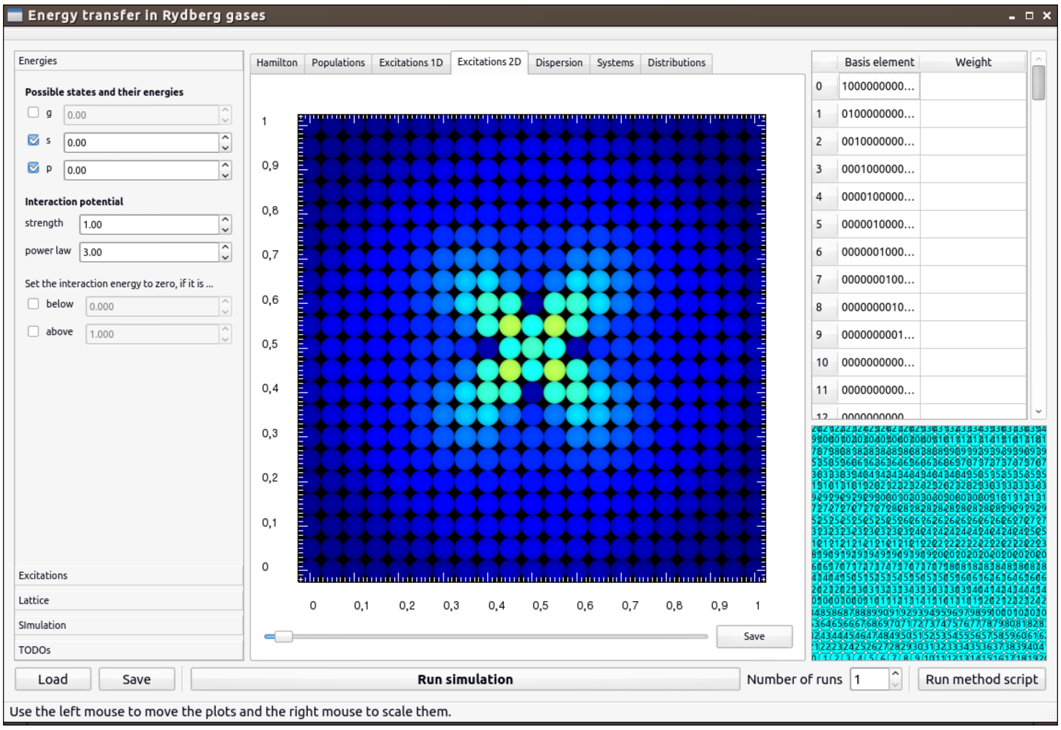

Energies

Possible states and their energies

☐ g 0.00

☑ s 0.00

☑ p 0.00

Interaction potential

strength 1.00

power law 3.00

Set the interaction energy to zero, if it is ...

☐ below 0.000

☐ above 1.000

	Basis element	Weight
0	1000000000...	
1	0100000000...	
2	0010000000...	
3	0001000000...	
4	0000100000...	
5	0000010000...	
6	0000001000...	
7	0000000100...	
8	0000000010...	
9	0000000001...	
10	0000000000...	
11	0000000000...	
12	0000000000...	

Number of runs 1

Use the left mouse to move the plots and the right mouse to scale them.

Fig. 3: Graphical user interface of the simulation program

In order to perform calculations, the users has to specify the system they like to simulate.

- Power law of interaction potential
- Geometry of the pattern
- Number of excitations and their initial distribution

This input data is used to automatically calculate the basis elements and the Hamilton operator of the system. Furthermore the initial conditions of the Schrödinger equation are determined from the initial distribution of the excitations. The Hamilton operator is stored as a sparse matrix. The initial conditions and the basis elements are memorized as sparse vectors. The expression “sparse” means that nulls are not stored explicitly. This saves a lot of storage space in main memory.

Once calculated, the Hamiltonian and the basis elements are cached to reduce the simulation time.

The time evolution is calculated by diagonalization of the Hamilton operator, see equation 3. Since diagonalization requires the costly eigendecomposition, it is slow for huge matrices. Hence, it is necessary to keep the matrices small.

We achieve this by the use of two tricks.

- We use not all basis elements of the Fock space. If we like to simulate the spread of m excitations, only the basis elements that contain exactly m excitations are relevant to us.
- We are analyzing the Hamilton operator. If it is built up by several blocks as shown in equation 8, the program will identify them. In this case the program will perform the calculations with the blocks.

There are even more tricks to think of.

- Highly symmetric systems lead to highly symmetric matrices. These can be simplified by changing to a basis set that fits the symmetry.
- Huge eigenvalues cause fast oscillations. On average they are irrelevant, especially they can not be measured. Therefore, such eigenvalues do not need to be determined.
- The time evolution can also be calculated by integration of the Schrödinger equation. For very large systems this is faster than diagonalization.

However, these methods are not implemented yet because for our purposes we do not need them. A 500×500 matrix is still diagonalized in roughly one second and we do not require larger ones.

3 Dependence on geometry and potentials

The objective of this chapter is to simulate and understand the energy transfer for several network geometries and interaction potentials. We start with simple networks. Thereafter we analyze lattices. Finally we end with random networks, that a hard to comprehend.

3.1 Simple networks

In the following a dipole-dipole interaction potential ($\propto 1/R^3$) is used for all patterns. We have chosen this particular potential because dipole-dipole interacting Rydberg atoms can be used to experimentally implement these networks. This is what we are going to look at in chapter 5.

All networks are plotted the same way.

- The particles are represented by spheres.
- Their color indicates the probability of finding an excitation in logarithmic scale. Blue stands for 0 and red for 1.

3.1.1 Dependence on number of neighbors

To figure out how position differences influence the propagation, we investigate several local network configurations.

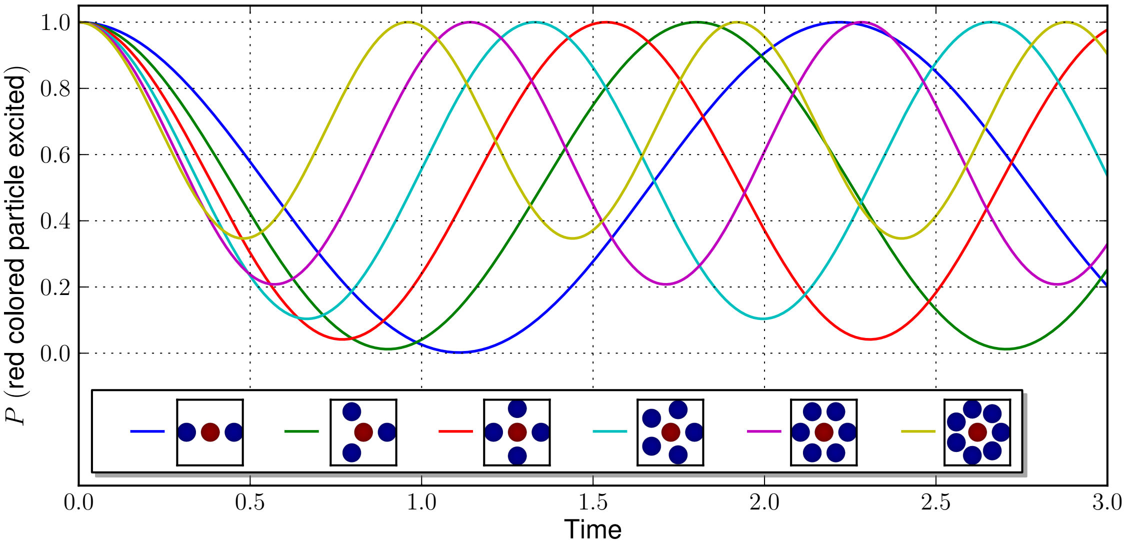

Fig. 4: At the beginning the central particles of the symmetric networks are excited. The plot shows the time evolution due to dipole-dipole interaction.

At first we like to study networks with one central particle that is surrounded by various neighbors. Initially the excitation is at the center. Because the neighbors are positioned symmetrically, the excitation propagates isotropically. Thus, the probability of finding a excitation is the same for all neighbors. Therefore all neighbors together behave like one virtual particle. Hence, all of these symmetric systems are comparable to two-particle systems and the excitation probabilities oscillate sinusoidally, see figure 4.

Increasing the number of the neighbors has two effects on the oscillating excitation probability.

1. The amplitude becomes small. A small amplitude means, that a minor percentage of the excitation leaves the central particle. Hence, for a huge number of neighbors the probability of finding the excitation in the center stays at a high level.
2. The frequency of the oscillation gets higher. The frequency increases so fast, that the following statement holds true: The more neighbors exist, the faster the excitation probability declines. Hence, if an excitation leaves the central particle, it will leave it very fast.

3.1.2 Dependence on distance between neighbors

Increasing the number of neighbors go along with reducing the distance between them. This raises the question whether the observations can also be made with two neighbors getting closer and closer to each other. The results are shown in figure 5.

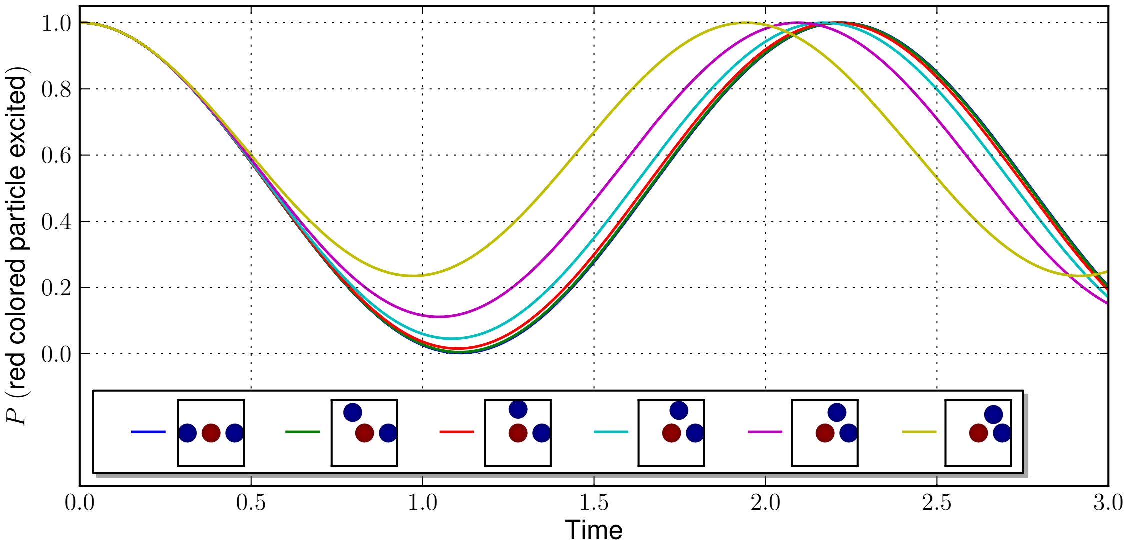

Fig. 5: An excited partical has two neighbors. Depending on the distance between the neighbors the excitation probability oscillates with a different amplitude and frequency.

As we can see, the amplitude becomes smaller and the frequency higher like it was observed before. However, the effect is much less pronounced. Additionally the excitation probability seems to decline with the same rate for all configurations. Thus an increase in the declining rate is a true many neighbor effect.

3.2 Regular lattices

After we have studied several simple network configurations we are going to analyze how the propagation depend on the type of interaction. In order to do this a linear chain, a cubic lattice, and a triangular lattice are studied with different interaction potentials. All lattices are finite, no periodic boundary conditions are applied.

We are going to use potentials which decreases as $1/R^\alpha$. The $1/R^{99}$-potential is a very good approximation for nearest neighbor interaction.

To ensure comparability between the lattices, as much of their parameters as possible are kept constant.

- The lattice constant $a = 1$ is the same in all directions.
- The linear chain consists of 21 particles. Both the cubic and the triangular lattice have 21×21 particles.
- All simulations start with one excitation in the middle of the lattice at $t = 0$. They end at $t = 4$

3.2.1 Linear chain

At the beginning we analyze the simplest possible lattice, the linear chain.

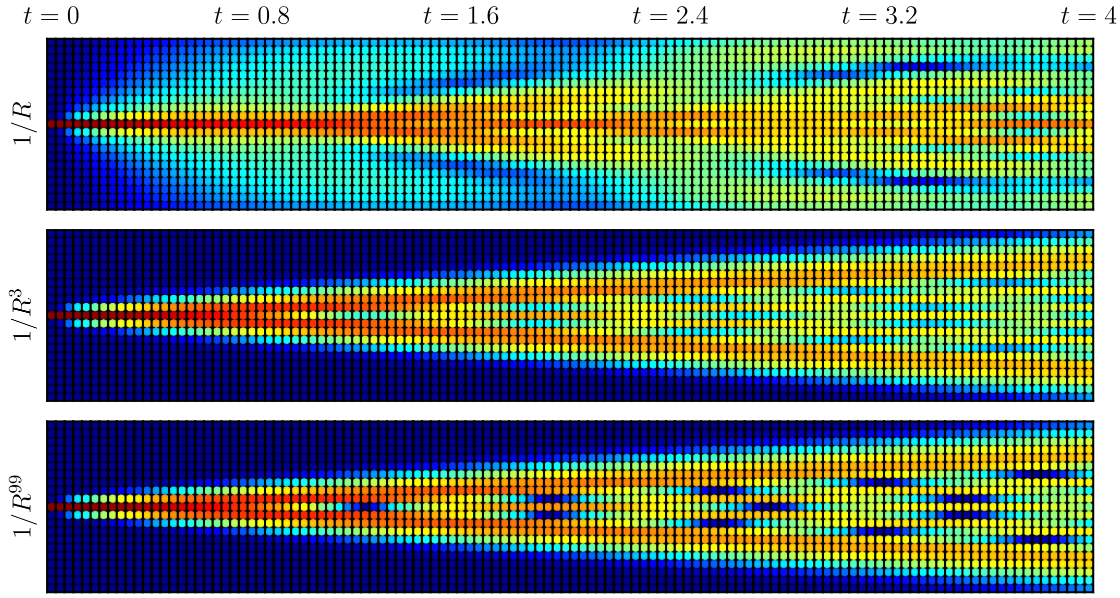

Fig. 6: The propagation of an excitation on linear chains is shown.

The $1/R$-potential completely differs from all other potentials (including $1/R^2$, although it is not shown). The excitation spreads much faster and interference fringes occur after a shorter time because of interaction with the boundary.[1]

The $1/R^{99}$-potential represents nearest neighbor interaction. Comparable systems have already been experimentally studied. For example, in a paper dealing with quantum walks of correlated photons [10] a similar model has been used. This shows the relationship to quantum walks, mentioned in chapter 1.

3.2.2 Cubic lattice

After the transition to the second dimension new effects occur. First of all excitations get distributed over a larger number of sites. The average probability of finding the excitation decreases.

Additionally, two-dimensional lattices are not isotropic — in contrast to the linear chain. As an example the cubic lattice is shown in figure 7.

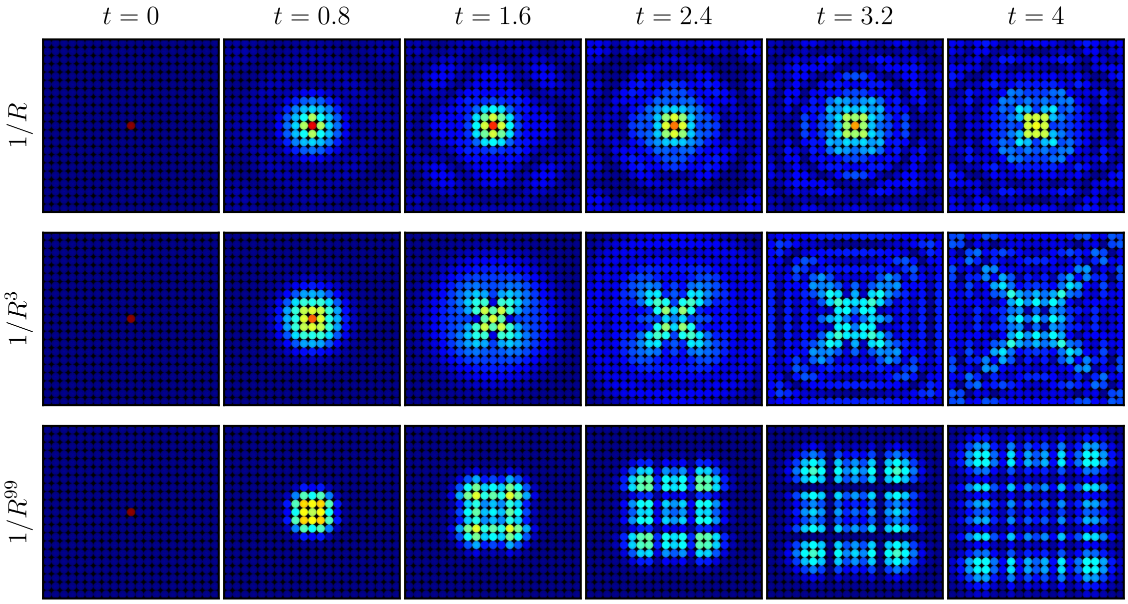

Fig. 7: The propagation of an excitation on cubic lattices is shown.

A particularly conspicuous aspect is, that the $1/R^3$-potential leads to dominant propagation along the diagonals. This is counterintuitive because the coupling along the diagonals is weaker than the coupling in the X- and Y-direction. Perhaps the phenomena could by understood by studying interference paths. The propagation along the diagonals does not occur for most of the other potentials.

---

[1] In chapter 4.1 we will learn about another fundamental difference between the $1/R$-potential and all others: For an infinite linear chain the dispersion relation diverges as k approaches zero.

It is also worth mentioning, that for the $1/R^3$-potential the inner interference pattern is surrounded by an isotropic bluish glow. We are going to explain its reason in chapter 4.4.

3.2.3 Triangular lattice

The triangular lattice is more isotropic than the cubic lattice. This is also reflected in the spread of the excitations, see figure 8. For example the $1/R^3$-potential leads to an almost isotropic propagation unless excitations get reflected by the boundary. We have to look closely to see phenomena similarly to the spread along the diagonals that occurred on cubic lattices.

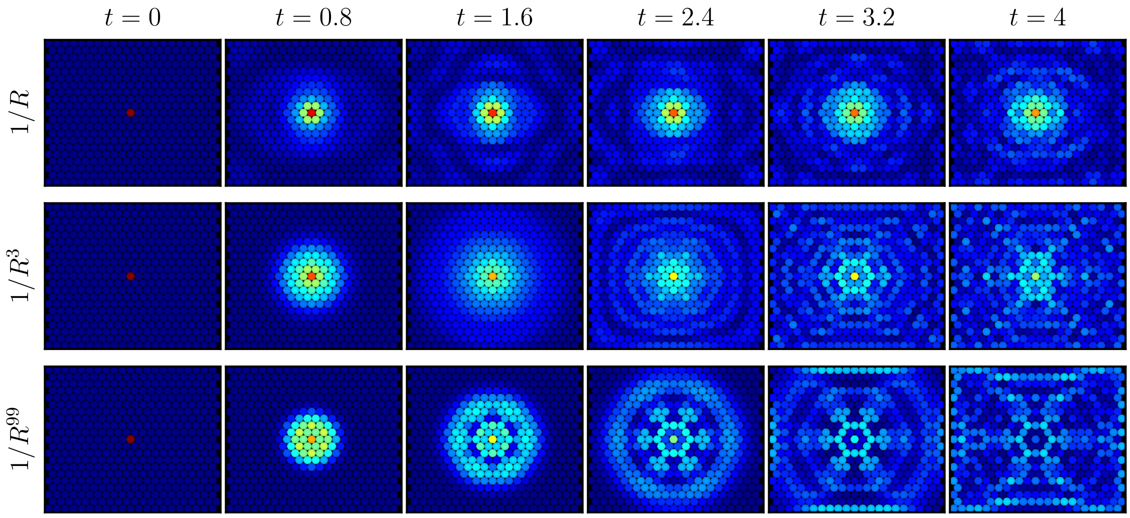

Fig. 8: The propagation of an excitation on triangular lattices is shown.

One can compare the speed of propagation between the lattices. We are going to do this for the $1/R^3$-potential. Thereto we can visually determine the time, when the outer bluish glow reaches the boundary. We obtain the following times:

- For the linear chain with coordination number 2: $t \approx 4$
- For the cubic lattice with coordination number 4: $t \approx 2.4$
- For the triangular lattice with coordination number 6: $t \approx 1.6$

As we can see, the higher the coordination number becomes, the faster one part of the excitation spreads.

Another part of the excitation stays at the central particle. The higher the coordination number becomes, the longer it stays. This is also illustrated by the comparison of the figures.

These observations are in in perfect agreement with the results of chapter 3.1.1.

3.3 Irregular patterns

Inspired by the assumption that nature uses quantum networks to transfer the energy of light [3], see chapter 1, we try to built up a network that transfers an excitation from a starting point to a goal.

As a first step to study such complex systems, we consider a small random network and then analyze the effect of small modifications of individual network site positions. Some results are shown in figure 9. As we can see, further optimization would be needed to obtain a really effective excitation transport. In order to do this genetic algorithms could be used [11].

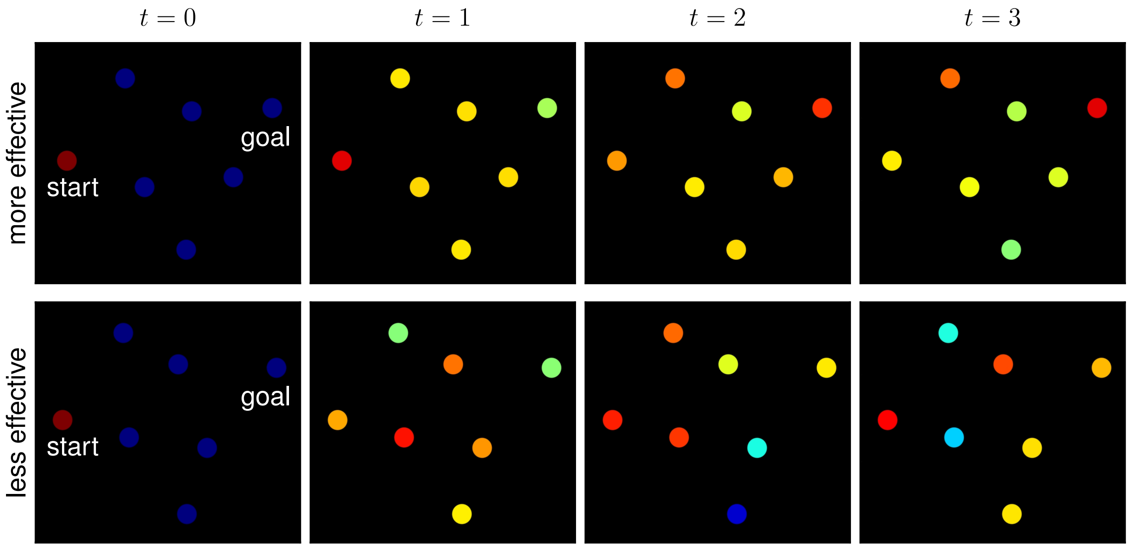

Fig. 9: The small position differences between the two patterns have a huge impact on the propagation. A dipole-dipole interaction potential is used.

4 Dispersion relations

Dispersion relations can provide a better understanding of the propagation of the excitations. Furthermore they can be determined analytically for simple models, for example for one-dimensional lattices in the shape of infinite linear chains. The results can be used to validate the simulation.

4.1 Analytic calculation

4.1.1 Linear chain with nearest neighbor interaction

A linear chain with nearest neighbor interaction was looked at. Let N be the number of sites and a the lattice constant. Then equation 5 takes the following form.

$$H = t \sum_{n=0}^{N-1} \left(c_n^\dagger c_{n+1} + c_n^\dagger c_{n-1} \right) \tag{9}$$

We assume that the lattice is periodic. Then the equation $c_n^{(\dagger)} = c_{n+j\cdot N}^{(\dagger)}$, $j \in \mathbb{Z}$ holds true for the creation and annihilation operators. They are located in the spatial domain and can be expressed by the use of the Fourier transformed operators $b^\dagger$ and b in the momentum domain with wave vector $k = \frac{2\pi}{a}\frac{j}{N}$, $j \in \{0, ..., N-1\}$ and $x_n = a \cdot n$.

$$c_n = \frac{1}{\sqrt{N}} \sum_k \exp(-ikx_n) \cdot b_k \tag{10}$$

$$c_n^\dagger = \frac{1}{\sqrt{N}} \sum_k \exp(ikx_n) \cdot b_k^\dagger \tag{11}$$

These expressions can be used to diagonalize the Hamilton operator.

$$\begin{aligned}
H &= \frac{t}{N} \sum_{n=0}^{N-1} \sum_{k,k'} \exp(ikx_n - ik'x_{n+1})\ b_k^\dagger b_{k'} + \exp(ikx_n - ik'x_{n-1})\ b_k^\dagger b_{k'} \\
&= \frac{t}{N} \sum_{n=0}^{N-1} \sum_{k,k'} \left(\exp(ikx_n - ik'x_{n+1}) + \exp(ikx_n - ik'x_{n-1})\right) \cdot b_k^\dagger b_{k'} \\
&= t \sum_{k,k'} [\exp(ik'a) + \exp(-ik'a)] \cdot b_k^\dagger b_{k'} \cdot \frac{1}{N} \sum_{n=0}^{N-1} \exp(i(k-k')x_n) \\
&= t \sum_{k,k'} [2\cos(k'a)] \cdot b_k^\dagger b_{k'} \cdot \exp(i\phi)\ \delta_{k-k'} \\
&= \sum_k [2t\cos(ka)] \cdot b_k^\dagger b_k \cdot \exp(i\phi) = \sum_k \epsilon(k) \cdot b_k^\dagger b_k \cdot \exp(i\phi)
\end{aligned} \tag{12}$$

The expression $\exp(i\phi)$ with the irrelevant phase ϕ was caused by the Fourier transform. It results in a phase shift, that can be neglected because of its global nature. We get the following dispersion relation [12].

$$\epsilon(k) = 2t\cos(ka) \tag{13}$$

4.1.2 Linear chain with $1/R^\alpha$-interaction

For other types of interactions the dispersion relation can be determined analytically with the help of the polylogarithm $\mathrm{Li}_s(z) = \sum_{n=1}^{\infty} \frac{z^n}{n^s}$ [13]. Let us assume the interaction strengths drops off as $1/R^\alpha$, so that we can use the hopping function $r(R) = 1/R^\alpha$. We like to look at a linear chain with $N+1$ sites. We define $x_n = a \cdot n$ with $n \in \{-N/2, ..., 0, ...N/2\}$ and lattice constant a. The function $\tilde{t}(R)$ reads as follows.

$$\tilde{t}(r) = \begin{cases} t(R) & R \neq 0 \\ 0 & R = 0 \end{cases} \tag{14}$$

With the help of this function and the creation and annihilation operators in momentum domain we can rewrite the Hamilton operator of the linear chain.

$$\begin{aligned} H &= \sum_{n \neq m} t(|x_n - x_m|)\; c_n^\dagger c_m \\ &= \sum_{k,k'} \frac{1}{N+1} \sum_{n \neq m} t(|x_n - x_m|) \exp(ikx_n - ik'x_m)\; b_k^\dagger b'_k \\ &= \sum_{k,k'} \frac{1}{N+1} \sum_{m} \exp(-ik'x_m)\; \sum_{n} \tilde{t}(|x_n - x_m|) \exp(ikx_n)\; b_k^\dagger b'_k \end{aligned} \tag{15}$$

We can use the shift theorem for discrete Fourier transform [14] and the definition of the delta function in Fourier space to get rid of the sum over m.

$$\begin{aligned} H &= \sum_{k,k'} \frac{1}{N+1} \sum_{m} \exp(i(k-k')x_m)\; \sum_{n} \tilde{t}(|x_n|) \exp(ikx_n)\; b_k^\dagger b'_k \\ &= \sum_{k,k'} \delta_{k-k'}\; \sum_{n \neq 0} t(|x_n|) \exp(ikx_n)\; b_k^\dagger b'_k \\ &= \sum_{k} \sum_{n=1}^{N/2} \left(\frac{\exp(ikx_n)}{|x_n|^\alpha} + \frac{\exp(-ikx_n)}{|x_n|^\alpha} \right)\; b_k^\dagger b'_k \end{aligned} \tag{16}$$

If the number of lattice sites N approaches infinity, we will obtain the polylogarithm. Here, $\mathrm{Re}\,[z]$ returns the real part of z.

$$H \to \sum_k \frac{2t}{a^\alpha}\, \mathrm{Re} \left[\sum_{n=1}^{\infty} \frac{\exp(ika)^n}{n^\alpha} \right]\; b_k^\dagger b_k = \sum_k \frac{2t}{a^\alpha}\, \mathrm{Re} \left[\mathrm{Li}_\alpha(e^{ika}) \right]\; b_k^\dagger b_k \tag{17}$$

This gives us the dispersion relation.

$$\epsilon(k) = \frac{2t}{a^\alpha}\, \mathrm{Re} \left[\mathrm{Li}_\alpha(e^{ika}) \right] \tag{18}$$

Its series expansion around $k = 0$ can be calculated for different α. Logarithms are extracted.

- for $\alpha = 1$: $\epsilon(k) = -2\,\log(|k|) + \mathcal{O}(|k|^2)$
  As we can see, this is a non-physical solution because it's divergent for $k = 0$.
- for $\alpha = 2$: $\epsilon(k) = \frac{\pi^2}{3} - \pi\;|k| + \mathcal{O}(|k|^2)$
- for $\alpha = 3$: $\epsilon(k) = 2\;\zeta(3) + |k|^2\;\log(|k|) + \mathcal{O}(|k|^2)$
- for $\alpha = 4$: $\epsilon(k) = \frac{\pi^4}{45} - \frac{\pi^2}{6}|k|^2 + \mathcal{O}(|k|^4)$
- for $\alpha > 4$: The leading term stays $|k|^2$.

The list is only valid for the one-dimensional case. The higher the number of dimensions become, the shorter the range of the potential has to be in order to get a quadratic dispersion relation for small k.

4.2 Determination from simulation data

The dispersion relation of a non-periodic cubic lattice can be determined by the use of the simulation program. One approach is to study the propagation of a Gaussian excitation $\Psi(r)$.

The Fourier transform of the Gaussian excitation is a Gaussian distribution $A(k)$ in k-space. In Fourier space the time evolution can be described with the help of the dispersion relation $\omega(k)$ [15].

$$\Psi(r,t) = \sum_k \;A(k)\;\exp(i(kr - \omega(k)t)) \tag{19}$$

It follows, that the discrete Fourier transformation of $\Psi(r,t)$ is a function of $\omega(k)$.

$$\mathrm{DFT}(\Psi(r,t)) \propto A(k)\;\exp(-i\omega(k)t) \tag{20}$$

Strictly speaking this equation holds true only for periodic boundary conditions. However, it can be seen as a good approximation for finite lattices, if the width of the excitation is much smaller than the lattice size. In this case one can make use of formula 20 to calculate the dispersion relation from the knowledge of the excitation at two different times t_1 and t_2.

$$\omega(k) = \ln\left(\frac{\mathrm{DFT}(\Psi(r,t_2))}{\mathrm{DFT}(\Psi(r,t_1))}\right)\;\frac{i}{t_2 - t_1} \tag{21}$$

In our simulation there is neither loss nor gain of excitations apart from effects caused by numerical errors. Hence, the imaginary part of ω is next to null. This is why we are going to plot only the real part of dispersion relations.

In practice we start the simulation at $t_1 = 0$ with one single excitation in the middle. So $\Psi(r,t_1)$ is a delta peak. Choosing it as the initial excitation has proofed useful because this approach minimizes the effect of the boundary. The time t_2, after which the excitation is determined again, has to be chosen thoughtfully. On the one hand a too short time prevents the excitation to feel the whole lattice and very small numbers occur, which evoke huge numerical errors. On the other hand a too long time leads to a broad excitation which interacts with the boundary. Moreover we have to watch out for different branches of the complex logarithm in equation 21.

We will have picked the right value of t_2, if small variations of this time have no influence on the obtained dispersion relation.

4.3 Comparison between simulation and analytic calculation

Several linear chains with different number of sites are studied. Either nearest neighbor interaction or a potential of the type $1/R^\alpha$ are used. The strategy described above is applied to determine the dispersion relation from simulation data. We make use of equation 13 and 18 to calculate the dispersion relation analytically for endless lattices. Because we work in atomic units the energies obtained from these formulas are equivalent to angular frequencies.

A comparison between the simulation results for 21 sites and the analytic calculations for an infinite number of sites is shown in figure 10. No free parameters are used.

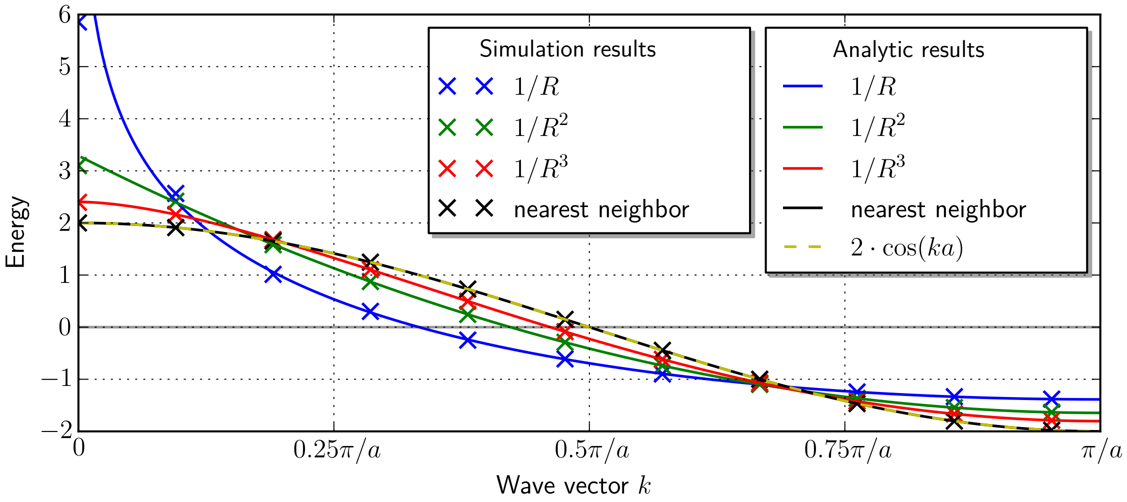

Fig. 10: The figure shows the dispersion relations of a linear chain for $1/R$-potentials as well as nearest neighbor interaction. We obtained dispersion relations for 21 sites from the simulation (shown as crosses). Analytical calculations resulted in dispersion relations for an infinite number of sites (shown as lines). Apparently the deviations between simulation and analytic results are negligible for huge wave vectors. For small ones finite size effects can occur.

The dashed yellow line represents the dispersion relation for nearest neighbor interaction that is expressed by equation 13. Instead of dealing with the exact expression one can use the potential $1/R^\alpha$ with a huge number α. This potential presents a very good approximation to the nearest neighbor potential. For calculating the black line we used $\alpha = 99$. No difference to the exact solution can be discerned.

The comparison between simulation and analytic calculation shows one obvious difference. The calculated dispersion relations are continuous. As opposed to this, the simulations yield wave vectors that can only attain discrete values because of the finite lattice size. Apart from that the results correspond very well, in particular for huge wave vectors k. For small k the deviations increase because small wave vectors means long wavelengths which strongly feel the boundary of the lattice. Hence, finite size effects occur. This becomes particular obvious for the $1/R$-potential. As shown in chapter 4.1 this potential will causes a divergent behavior for small k, if the lattice is endless. In our simulations only finite values occur.

In the following we like to examine the influence of the finite lattice size in detail. For this purpose the deviation between simulation and analytic results is determined for different number of lattice sites. As a measure for the deviation between calculated and simulated dispersion relations the absolute differences are determined at every point except $k = 0$. The values at this position are not used, because here the analytically calculated dispersion relation diverges for $1/R$.

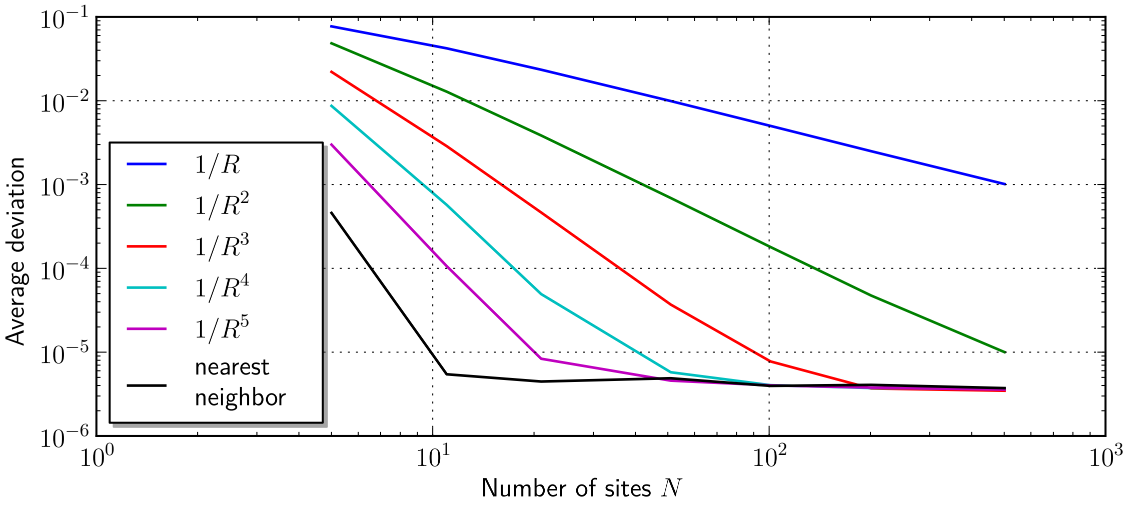

Fig. 11: This log-log plot shows the average deviations between simulated and analytically calculated dispersion relations for several $1/R^\alpha$-potentials as well as nearest neighbor interaction. The values at $k = 0$ are not taken into account because of the divergent behavior for $1/R$. All analytically calculations were accomplished with infinite lattices, whereas the simulations were performed on lattices with N sites. The graphs show that finite-size effects will decrease very fast, if small lattices grow in size.

The average deviations are shown in figure 11 as a function of the number of sites N. The straight lines in this log-log plot indicate that the average deviations decreases as $\frac{1}{N^m}$ for small numbers N. The slopes of the lines tell us that the constant m attains values between 0.8 for the $1/R$-potential and 5.6 for nearest neighbor. The shorter the range of the interaction potential is, the faster the average deviation decrease.

No matter what potential is present the deviation decrease the fastest for small number of sites. This allows us to use our analytic models already for a small lattices provided that we don't want to study any divergent behavior.

Let us compare the magnitude of the deviations with the relevant energy scales. As we can see in figure 10 the energies are within the single-digit range for all wave vectors. Already for five sites the deviations are one to three orders of magnitude smaller. They bottom out at 10^{-6}. This number represents the deviation caused by numerical errors.

All in all there is a good agreement between the numerical models for endless lattices and the simulation results for finite ones. Therefore we can assume that the simulation provides valid results.

4.4 Analysis of several dispersion relations

After we have validated the simulation program with analytic results, we are going to use it to obtain further dispersion relations. They will help us understand the propagation of excitations.

In the following we are going to study two-dimensional cubic lattices. Therefore the momentum space and so the dispersion relation have two dimensions. As an example the dispersion relation of a 21×21 lattice with a $1/R^3$ interaction potential is visualized by a color map, see figure 12. It shows that the dispersion relation is isotropic only for small wave vectors. The reason for this is that a huge wave vector is equivalent to a small wavelength, which feels the anisotropy of the cubic lattice.

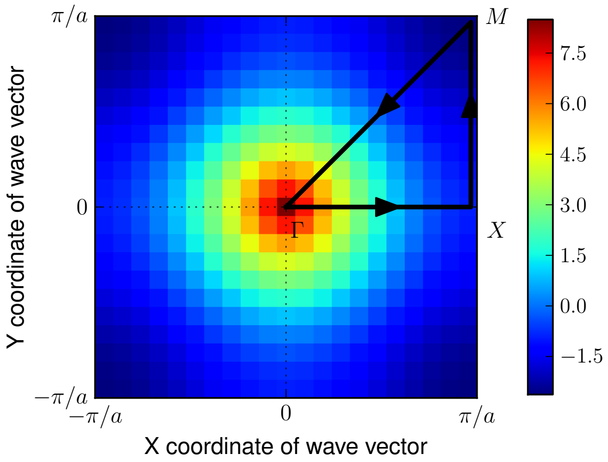

Fig. 12: The image shows the dispersion relation for a two-dimensional cubic lattice with the interaction potential $1/R^3$. The bigger the wave vector is the more anisotropic the dispersion relation becomes. The black lines display the way along which several two-dimensional dispersion relations are plotted in figure 13.

Instead of using color maps one can plot the dispersion relation along straight lines connecting characteristic points of the two-dimensional dispersion relation. In doing so one can show several dispersion relations in the same diagram. This enables us to compare them. Figure 13 shows the dispersion relation as well as the absolute values of the corresponding group velocities. They can be calculated with the following formula.

$$v_{\text{group}} = \left| \frac{\mathrm{d}\omega(k)}{\mathrm{d}k} \right| \tag{22}$$

Because we are in atomic units angular frequencies are equivalent to energies and we obtain the group velocities as slopes of the graphs in the upper diagram of figure 13.

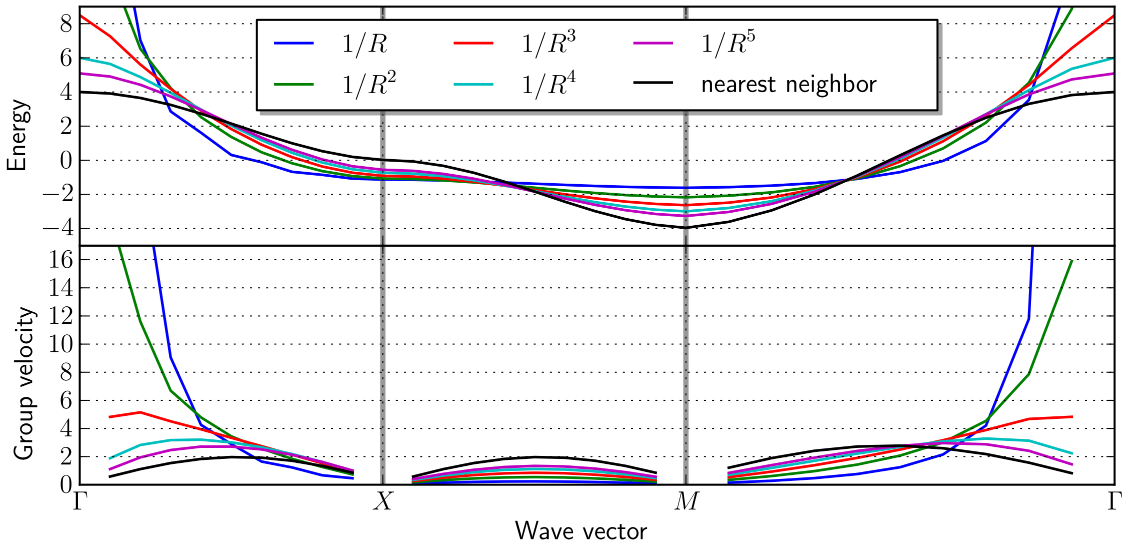

Fig. 13: In the upper diagram the two-dimensional dispersion relations for nearest neighbor and $1/R^{\alpha}$ interaction potentials are plotted along straight lines connecting the symmetry points shown in figure 13. The lower diagram visualizes the absoulte values of the corresponding group velocities. The used lattice has 21×21 sites.

This figure hints at several properties of the dispersion relations.

- All dispersion relations have in common that the energy reaches its maximum at $k = 0$. The first energetic minimum is at $k_{x,y} = \pi/a$. Why this is the case, can be explained using the example of a dipole-dipole interaction potential.[2] Suppose that there is a dipole at each site of the two-dimensional lattice. Since the wavelength equals infinity for $k = 0$ all dipoles are orientated in the same direction. Thus the dipoles repulse each other and the interaction energy is high. For $k_{x,y} = \pi/a$ the wavelength equals $\lambda = \frac{2\pi}{k} = a/2$, so that the dipoles are orientated alternately up or down. Hence, each dipole attracts its nearest neighbors. Therefore the interaction energy is below zero.

---

[2] A detailed discussion of the dipole-dipole potential is provided in chapter 5.1.

- The longer the range of a potential is, the higher maximum group velocities occur. This finding matches the observation that excitations spread faster with long range than with short range interactions.
- For short range interactions the highest group velocities are located on the diagonal of the dispersion relation. This is particularly true for nearest neighbor interaction. This result is somewhat counter-intuitive because a nearest neighbor potential prevents direct interactions between diagonally adjacent sites. So an excitation can get from one site to its diagonal neighbors only by choosing a detour. Perhaps interference is the key to understanding why the propagation along the diagonal is still so fast.

Now, we like to take a detailed look at the influences of a dispersion relation on the propagation of several Gaussian excitations. We study a two-dimensional cubic lattice with the dipole-dipole interaction potential $1/R^3$. We have decided to use this potential, because we are going to deal with it extensively in chapter 5.

At the beginning of our simulation the particles in the middle of a lattice with 21×21 sites share one excitation. The probability to find the excitation is Gaussian distributed. We are going to examine the influence of the width of the excitation on their propagation behavior. Therefore we are going to use excitations in the form of a delta peak as well as a small and broad Gaussian distribution. Figure 14 shows these peaks in Fourier space along with the dispersion relation.

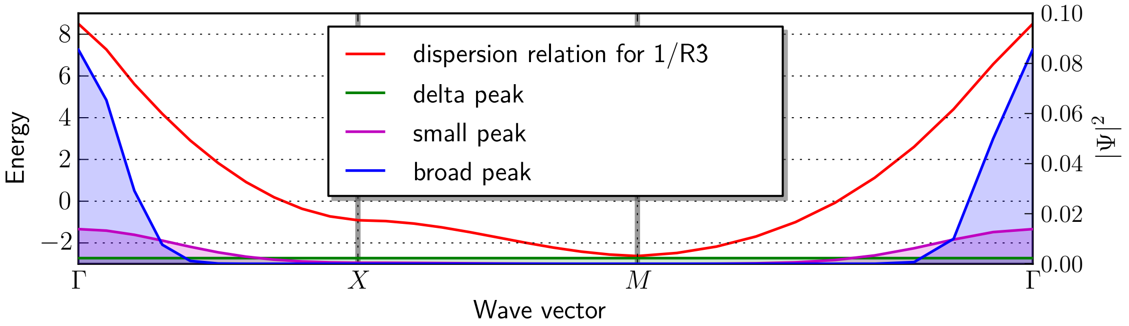

Fig. 14: The smaller a excitation in position space is the broader it gets in momentum space. Hence a delta excitation feels the whole dispersion relation. In contrast, a broad Gaussian excitation is influenced only by the dispersion relation for small wave vectors.

It demonstrates that depending on the widths of the peaks other parts of the dispersion relation are relevant to them. For instance, the delta peak feels the whole dispersion relation because it's infinitely broad in momentum space.

As we have seen in figure 12 the dispersion relation is isotropic for small wave vectors. A Gaussian distribution that is broad in position space does only contain small wave vectors. Therefore one expects, that such an excitation propagates in an isotropic manner. It is even possible to predict the propagation in greater detail. As figure 14 shows, the dispersion relation is nearly linear for small wave vectors.[3] Hence on anticipates that the broad excitation propagates circularly in all directions with a constant velocity like a ring of light. As we can see in figure 15 these expectations are correct.

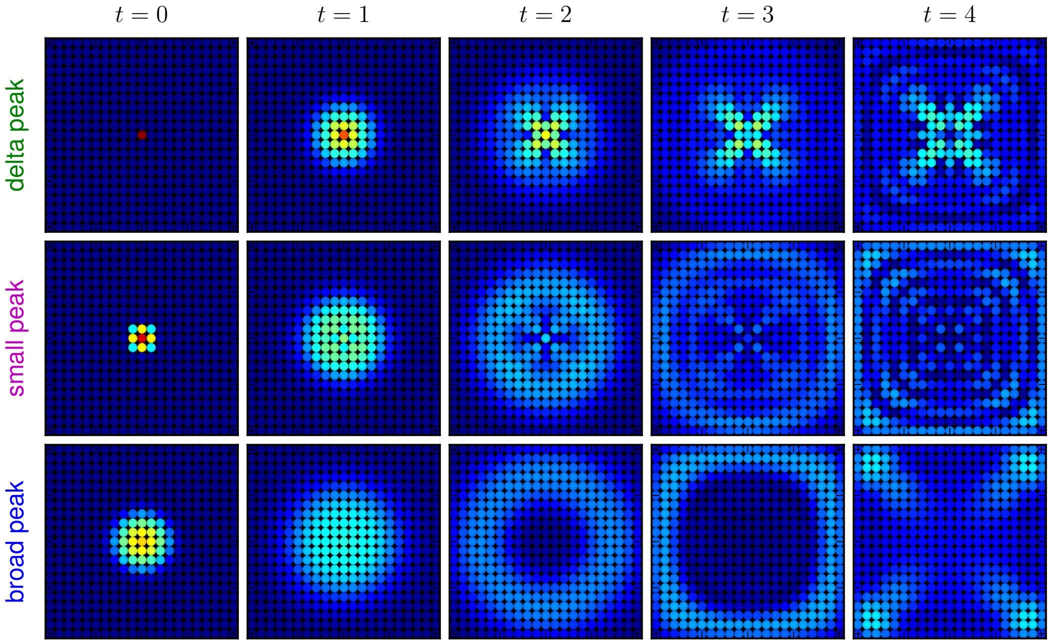

Fig. 15: The figure shows two-dimensional lattices with 21×21 sides and $1/R^3$ interaction potentials (logarithmic color scale). At the time $t = 0$ several Gaussian distributions are excited. Depending on their width they see different parts of the dispersion relation and propagate in different ways. From the time $t = 3$ on the excitations interact with the boundaries. Hence phenomena like standing waves can be observed.

The propagation of a small or even delta shaped peak can not be easily predicted from the dispersion relation. However, some general statements can be made based on figure 15.

- The part of the excitation that feels the isotropic section of the dispersion relation spreads homogeneously. The propagation is fast, because the isotropic section contains the highest group velocities, see figure 13.
- The other part of the excitation propagates anisotropically and slowly. We can see interference phenomena.

Interaction with the boundaries of the lattice leads to interference pattern. Here, another difference between small and broad peaks can be observed. For small peaks the distance between interference fringes is smaller than for broad peaks. The reason for this is, that broad peaks lack huge wave vectors and thus small wavelengths.

---

[3] In chapter 4.1 we saw that a $1/R^2$-potential and not a dipole-dipole potential leads to a linear dispersion relation for small wave vectors. However, this result was obtained by looking at one-dimensional lattices.

5 Implementation with superatoms

In chapter 3, we have simulated excitonic energy transfer. To realize it experimentally one could make use of ultracold Rydberg atoms in the s and p-state as interacting two-level systems. Another proposal is to use so-called superatoms, which are caused by the Rydberg blockade [16]. In the current chapter, we are going to analyze how promising this approach is.

Before we can start with the analysis, we have to explain what superatoms are. In order to do this we need to know about Rydberg atoms and their interaction.

5.1 Rydberg atoms

A Rydberg atom is an atom, that have one electron excited to a very high principal quantum number n. The excited electron feels a hydrogenic potential due to its large distance from the nucleus and the core electrons [17].

It can be described by formulas much in the same way as the hydrogen atom. One can derive scaling laws of several atomic properties by the use of these equations.

Property	Scaling law
Polarizability	n^7
Dipole matrix elements between neighboring levels	n^2
Radiative life time	n^3

Tab. 1: Most atomic properties of Rydberg atoms depend on the principle quantum number n. This table shows the scaling laws [18] of properties that are relevant for us.

As we can see, Rydberg atoms are strongly interacting because of their high quantum number n. This facilitates exciting experiments.

In the following we are going to work with a simple model of an atom.

- The atom can be in the ground state, Rydberg s-state or p-state.
- The dipole matrix element between the ground state and a Rydberg state is negligibly small. Transitions between the ground state and a Rydberg state won't occur at least unless they are externally driven.
- The dipole matrix element between the Rydberg s-state and p-states is huge.

In our simulation we are going to use several of these atoms. Since the dipole matrix elements scale with n^2, there is a strong dipole-dipole interaction between an atom in a Rydberg s-state and one in a Rydberg p-state (ground state atoms can be neglected).

To determine the Hamilton operator for dipole-dipole interaction we take the classical expression for the interaction energy as a starting point. For two classical dipoles $\vec{d_1}$ and $\vec{d_2}$ at a distance of $\vec{r}$ the energy in atomic units can be calculated with the following formula [19].

$$E = \frac{\vec{d}_1 \cdot \vec{d}_2 - 3(\vec{d}_1 \cdot \hat{\vec{r}})(\vec{d}_2 \cdot \hat{\vec{r}})}{|\vec{r}|^3} \tag{23}$$

To simplify this formula we like to get rid of the angular dependency. For that reason we assume that the dipoles are aligned parallel and the distance vector $\vec{r}$ is perpendicular to $\vec{d}_1$ and $\vec{d}_2$.

$$E = \frac{d_1 \cdot d_2}{|\vec{r}|^3} \tag{24}$$

This classical equation can be transformed into a quantum formula. Seen as a special case of a two-body interaction the dipole-dipole interaction can be easily noted in second quantization. In order to do this indices q, r, s and t are used. Each index indicates the state of an atom. It can be seen as a multi-index which tells us the atom position and whether the atom is in the s-state or p-state: $q = \{\text{position}, \text{s-state or p-state}\}$.

The dipole matrix element $d = \left| \langle q \mid \hat{d} \mid s \rangle \right|$ will occur in the following formula. It's non-zero only for transitions between the s-state and the p-state. Therefore we have to sum up only over particular indices.

$$\begin{aligned} H_{dip} &= \sum_{q,r,s,t} \langle q, r \mid \text{classical dipol-dipol interaction energy } E \mid s, t \rangle \; b_q^\dagger b_r^\dagger b_t b_s \\ &= \sum_{a \neq b} \frac{d^2}{{r_{ab}}^3} \; b^\dagger_{\{a,\text{s-state}\}} b^\dagger_{\{b,\text{p-state}\}} b_{\{a,\text{p-state}\}} b_{\{b,\text{s-state}\}} \end{aligned} \tag{25}$$

This equation can be simplified. The atom at position a will be in state $\{a, \text{p-state}\}$, if and only if it isn't in state $\{a, \text{s-state}\}$. Hence, it's enough to store whether the atom is excited in the p-state. Therefore the Fock space of the atoms can be reduced to the Fock space of excitations, which we have introduced in chapter 2.2.

To simplify equation 25, let us define new operators $c_a^\dagger = b^\dagger_{\{a,\text{s-state}\}} b_{\{a,\text{p-state}\}}$ and $c_a = b^\dagger_{\{a,\text{p-state}\}} b_{\{a,\text{s-state}\}}$. They operate in the Fock space of excitations and fulfill the commutation relations of hard-core bosons [20].

$$[c_a^\dagger, c_b^\dagger] = [c_a, c_b] = [c_a, c_b^\dagger] = 0 \text{ for } a \neq b$$

$$\{c_a^\dagger, c_a^\dagger\} = \{c_a, c_a\} = 0 \tag{26}$$

$$\{c_a, c_a^\dagger\} = 1 \tag{27}$$

These commutation relations result from the bosonic commutation relations for $b^{(\dagger)}$ and the fact, that an atom can be either in the p-state or in the s-state.

With the new operators equation 25 gets its final form. It resembles equation 5 for dipol-dipol interaction.

$$H_{dip} = \sum_{a \neq b} \frac{d^2}{{R_{ab}}^3} \; c_a^\dagger c_b \tag{28}$$

This shows, our strongly interacting Rydberg system is a special case of the universal model we have analyzed before. On the first glance it seems perfectly suited to experimentally study excitonic energy transfer. However, in practice it is hardly possible to excite single atoms to Rydberg states. Instead of single Rydberg atoms one obtains superatoms. In the following we are going to explain it.

5.2 Superatoms

Let us assume we try to excite atoms inside a dense cloud to Rydberg states with the help of a laser.

The van der Waals interaction between Rydberg atoms is very strong because of their high polarizability. The interaction shifts the energy levels of the atoms. If the shift is greater than the bandwidth of the excitation laser, the laser will be out of resonance and the atoms can not be excited. Hence, if one atom is in a Rydberg state, no further atoms can be excited in its surrounding volume. This mechanism is referred to as Rydberg blockade.

Since one can not tell which atom was firstly excited, the correct quantum state is a superposition of all possibilities. We can imaging a cluster of atoms sharing one excitation. This cluster is called superatom [17].

If we neglect the internal structure of superatoms, they are similar to normal atoms. If this approximation is valid, we will have a tool to experimentally study the mechanisms of excitonic energy transfer. We are going to determine the limits of this approximation with the help of simulations.

5.3 Simulation procedure

For this purpose we look at a system consisting of two superatoms. The right one is in the collective Rydberg s-state and the left one excited to the collective Rydberg p-state. If they behaved like normal atoms, the probability P of finding the excitation on the left hand side would be a cosine function of time. The probability could be calculated by diagonalization of the Schrödinger equation as described in chapter 2.1. In atomic units, it could be expressed by the following formula where E is the interaction energy.

$$P = \frac{1}{2}\left(\cos(2Et) + 1\right) \tag{29}$$

To figure out whether this is indeed the case we have to calculate the exact time evolution of our superatom system. In order to do this one has to use a basis set that represents all possible many-particle states. Lets assume that both superatoms consists of N atoms. Then each basis element can be expressed by a vector with $2N$ elements.

$$(a_1, ...a_N, b_1, ...b_N)^T \tag{30}$$

Here, a_i (resp. b_i) stands for the quantum state of the atom that is located at the site i of the superatom a (resp. b). For the following notations we introduce indices $x \in \{a, b\}$ and $y \in \{a, b\}$.

There are three possible quantum states for each atom.

- Ground state: $x_i = -1$
- Rydberg s-state: $x_i = 0$
- Rydberg p-state: $x_i = 1$

Since both superatoms can contain only one Rydberg state each, all but one x_i have to be -1. This consideration reduces the size of our basis set enormously.

Let us suppose the superatom a is in the collectively Rydberg p-state and b is in the collectively Rydberg s-state. Then we have to choose the following start vector.

$$|\Psi_{start}\rangle \propto \begin{pmatrix} a_1 = 1 \\ a_2 = -1 \\ a_3 = -1 \\ \vdots \\ b_1 = 0 \\ b_2 = -1 \\ b_3 = -1 \\ \vdots \end{pmatrix} + \begin{pmatrix} 1 \\ -1 \\ -1 \\ \vdots \\ -1 \\ 0 \\ -1 \\ \vdots \end{pmatrix} + \begin{pmatrix} 1 \\ -1 \\ -1 \\ \vdots \\ -1 \\ -1 \\ 0 \\ \vdots \end{pmatrix} + \begin{pmatrix} -1 \\ 1 \\ -1 \\ \vdots \\ 0 \\ -1 \\ -1 \\ \vdots \end{pmatrix} + \dots \tag{31}$$

For our system containing two superatoms the Hamilton operator 28 has to be slightly modified.

$$H_{super} = \sum_{x_i \neq y_j} \begin{cases} 0 & x_i = -1 \lor y_i = -1 \\ \frac{d^2}{{R_{x_i y_j}}^3} \, c_{x_i}^\dagger c_{y_j} & \text{otherwise} \end{cases} \tag{32}$$

If we look carefully at the Hamilton operator and the basis set, we will make an interesting observation: For each basis element $|\Psi_i\rangle$ there is exactly one other basis element $|\Psi_j\rangle$, so that $\langle \Psi_i \mid H_{super} \mid \Psi_j \rangle \neq 0$. This means the Hamilton operator is composed of 2×2 matrices. Thus the Schrödinger equation separates into equations for pairwise interacting particles!

Hence, we do not need to perform simulations with superatoms. It is sufficient to do the simulations with normal atoms for several times. At each run we have to select one atom from every superatom. We have to proceed until every possible atom combination has been selected. In the end we have to average over the complex results of each run. This gives us the time evolution of the superatom system.

5.4 Simulation results

For the simulation we suppose that the atoms inside each superatom are uniformly distributed. We use the width of the distribution as a measure of the diameter of the two superatoms. In figure 16 the results are plotted. We averaged over several runs until the shape of the curves did not change any more.

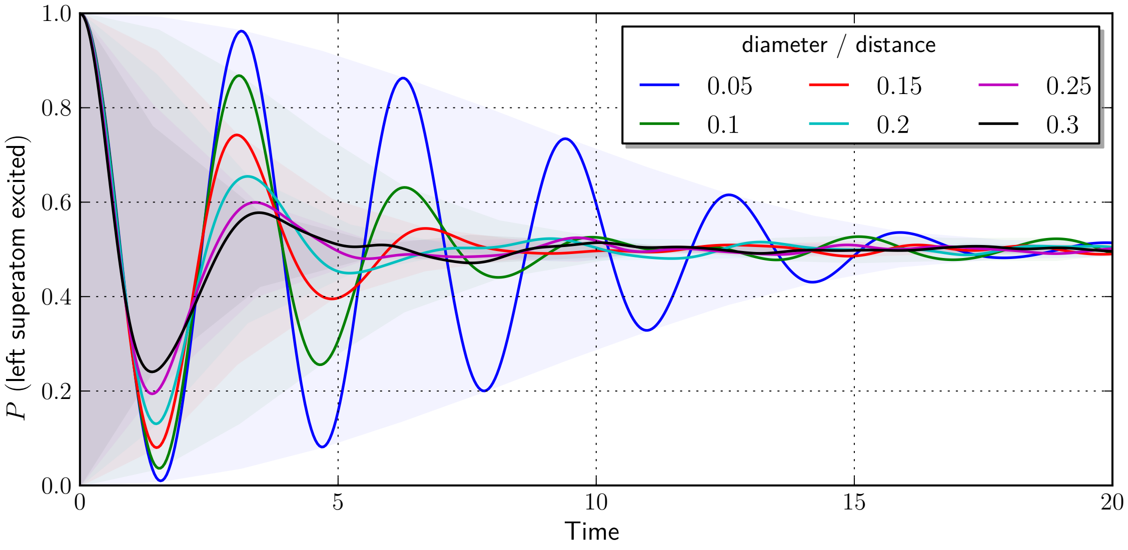

Fig. 16: The coherent time evolution of systems consisting of two superatoms is plotted. The colored areas symbolise the decline of the amplitudes over time.

As we can see, the time evolution strongly depends on the diameter of the superatoms in comparison to their distance. For a small diameter the superatoms behaves similarly to normal atoms. The excitation is transferred from one superatom to the other one and back again. For an increasing diameter the oscillation is damped more and more. Less oscillations can be seen. For example, for a diameter one tenth the small as the distance we observe roughly three oscillations. The reason for this decay is that the atoms of the superatoms couple pairwise. Because of the physical extension of the superatoms the coupling strength varies. This leads to oscillations with several frequencies. On average we obtain curves that seem to be damped. However, if the curves have approached zero and we wait for some time, we will see an revival of the oscillations. This phenomenon is characteristic for dephasing.

6 Conclusion and outlook

Conclusion

We analyzed networks of bosons coupled by $1/R^{\alpha}$-potentials. The interactions led to propagation of excitations.

At the beginning of the work we developed a general model describing the dynamics in such networks. The software programmed during this thesis implements the model and solves the resulting Schrödinger equation efficiently. Its graphical user interface enables easy setup of network geometries and interaction potentials.

To develop a general understanding of the basic exchange action we first studied simple networks containing only few sites. In doing so we got the result, that increasing the number of neighbors of an excited particle has two effects. Firstly, a higher percentage of the excitation stays at the particle. Secondly, the percentage of the excitation which does not stay leaves it faster. After we had understood the simple systems we looked at more complicated ones. Two-dimensional regular lattices reveal interesting phenomena because of their anisotropy. For example, on a cubic lattice with dipole-dipole interaction the excitation spreads along the diagonals. Finally we considered random networks. It turned out that already small modifications of individual network site positions have a huge impact on the propagation. Thus it is a hard job to design networks that lead to targeted propagation of excitations. However, as previously said photosynthetic organisms managed to efficiently transfer light energy through quantum networks. This energy transfer is subject of active research [3, 5].

To validate our simulation procedure we analytically calculated dispersion relations for linear chains and compared them to simulation results. Even though the calculations were performed with infinite chains and the simulation with finite ones, both results matched very well — except for some finite-size effects: In case of finite chains the wave vector can only attain discrete values and no divergent behavior can occur. Dispersion relations can also provide a better understanding of the propagation of excitations in cubic lattices. The dispersion relation is isotropic only for small wave vectors. Hence, only the long-wave Fourier components of an Gaussian excitation propagate isotropically. Additionally we calculated and discussed group velocities.

In the end we analyzed the feasibility of experimentally studying excitonic energy transfer with so-called superatoms. In order to do this we looked at systems consisting of two superatoms. We figured out, that the Schrödinger equation separates into equations for pairwise interacting particles. Thus the time evolution could be calculated by simulating several two particle systems. We saw that superatoms behave approximately the same way as normal atoms. However, their physical extension causes dephasing. This means, in principle we can use superatoms to study excitonic energy transfer, but we have to keep their diameter small in comparison to their distance. Otherwise we will hardly observe anything due to the fast dephasing.

Outlook

One future goal is to experimentally realize the simulated systems with superatoms.

There are also a lot of further theoretical questions.

- How does disorder, perturbation of energy levels, and decoherence [21] influence the propagation of excitations?
- Is it possible to use these effects to obtain more effective energy transfer?
- Which network geometry allows the most effective transport?

To answer the last two questions one would have to investigate many different network configurations. Probably it would be possible to construct theories for large classes of networks. Another approach would be to let the computer systematically examine a great many configurations. This could be done for example by the use of genetic algorithms [11].

List of tables

List of figures

References

[1] T. J. Osborne and N. Linden, “Propagation of quantum information through a spin system,” *Physical Review A*, vol. 69, no. 5, p. 052315, 2004.

[2] T. J. Apollaro, S. Lorenzo, and F. Plastina, “Transport of quantum correlations across a spin chain,” *International Journal of Modern Physics B*, vol. 27, no. 01n03, 2013.

[3] G. S. Engel, T. R. Calhoun, E. L. Read, T.-K. Ahn, T. Mančal, Y.-C. Cheng, R. E. Blankenship, and G. R. Fleming, “Evidence for wavelike energy transfer through quantum coherence in photosynthetic systems,” *Nature*, vol. 446, no. 7137, pp. 782–786, 2007.

[4] H. Gersch and G. Knollman, “Quantum cell model for bosons,” *Physical Review*, vol. 129, no. 2, p. 959, 1963.

[5] F. Perrin, “Théorie quantique des transferts d’activation entre molécules de même espèce. cas des solutions fluorescentes,” *Ann. Phys.(Paris)*, vol. 12, pp. 283–314, 1932.

[6] A. M. Childs, R. Cleve, E. Deotto, E. Farhi, S. Gutmann, and D. A. Spielman, “Exponential algorithmic speedup by a quantum walk,” in *Proceedings of the thirty-fifth annual ACM symposium on Theory of computing*, pp. 59–68, ACM, 2003.

[7] A. M. Childs, D. Gosset, and Z. Webb, “Universal computation by multiparticle quantum walk,” *Science*, vol. 339, no. 6121, pp. 791–794, 2013.

[8] A. Ben-Shem, F. Frolow, and N. Nelson, “Evolution of photosystem i–from symmetry through pseudosymmetry to asymmetry,” *FEBS letters*, vol. 564, no. 3, pp. 274–280, 2004.

[9] A. Ahmadi, R. Belk, C. Tamon, and C. Wendler, “Mixing in continuous quantum walks on graphs,” *arXiv preprint quant-ph/0209106*, 2002.

[10] A. Peruzzo, M. Lobino, J. C. Matthews, N. Matsuda, A. Politi, K. Poulios, X.-Q. Zhou, Y. Lahini, N. Ismail, K. Wörhoff, *et al.*, “Quantum walks of correlated photons,” *Science*, vol. 329, no. 5998, pp. 1500–1503, 2010.

[11] M. Melanie, “An introduction to genetic algorithms,” *Cambridge, Massachusetts London, England, Fifth printing*, vol. 3, 1999.

[12] F. Essler, *The One-Dimensional Hubbard Model*, pp. 22–23. Cambridge University Press, 2005.

[13] Wikipedia contributors, “Polylogarithm. Wikipedia, The Free Encyclopedia.” `http://en.wikipedia.org/w/index.php?title=Polylogarithm&oldid=568408173`. Accessed: August 16, 2013.

[14] Wikipedia contributors, “Discrete Fourier transform. Wikipedia, The Free Encyclopedia.” `http://en.wikipedia.org/w/index.php?title=Discrete_Fourier_transform&oldid=571363256`. Accessed: September 12, 2013.

[15] C. Cohen-Tannoudji, B. Diu, and F. Laloë, *Quantenmechanik*, p. 49. Walter De Gruyter Incorporated, 2009.

[16] R. Côté, A. Russell, E. E. Eyler, and P. L. Gould, "Quantum random walk with rydberg atoms in an optical lattice," *New Journal of Physics*, vol. 8, no. 8, p. 156, 2006.

[17] R. Löw, H. Weimer, J. Nipper, J. B. Balewski, B. Butscher, H. P. Büchler, and T. Pfau, "An experimental and theoretical guide to strongly interacting rydberg gases," *Journal of Physics B: Atomic, Molecular and Optical Physics*, vol. 45, no. 11, p. 113001, 2012.

[18] T. Gallagher, *Rydberg Atoms*, p. 25. Cambridge Monographs on Atomic, Molecular and Chemical Physics, Cambridge University Press, 2005.

[19] J. Jackson, C. Witte, and K. Müller, *Klassische Elektrodynamik*, p. 176. Überarbeitete Auflage, Gruyter, Walter de GmbH, 2006.

[20] P. T. T. NGA and N. T. THANG, "Supersolids of hardcore–bosons on a triangular lattice," in *Proc. Natl. Conf. Theor. Phys*, vol. 35, pp. 175–182, 2010.

[21] V. Kendon and B. Tregenna, "Decoherence can be useful in quantum walks," *Physical Review A*, vol. 67, no. 4, p. 042315, 2003.

Danksagung

Zum Schluss möchte ich allen danken, die zum Gelingen dieser Bachelorarbeit beigetragen haben. Ich danke ...

- *Professor Tilman Pfau* für die Ermöglichung der Bachelorarbeit und seine interessante Atomphysikvorlesung.
- *Sebastian Hofferberth* und *Robert Löw* für die tolle Betreuung und die ausführlichen Diskussionen.
- *Professor Hans Peter Büchler* und *David Peter* aus dem benachbarten theoretischen Institut für viele Anregungen und nützliche Tipps.
- dem *5. Physiklischen Institut* für die Talks und die Einblicke in die Versuche.
- *April Cooper* für das Korrekturlesen meiner Bachelorarbeit.
- *Jan Kumlin* und *Hannes Seeger* für die letzten Jahre und die tiefschürfenden Gespräche beim Mitagessen.
- meiner *Familie* und *Nina* für die Korrekturhinweise.